

Brillouin Scattering in Cubic Crystals*

G. B. BENEDEK AND K. FRITSCH†

*Department of Physics, Spectroscopy Laboratory, and Center for Materials Science and Engineering,
Massachusetts Institute of Technology, Cambridge, Massachusetts*

(Received 16 March 1966)

Using a helium-neon laser light source and a high-resolution grating spectrograph we have studied, at room temperature, the Brillouin spectrum of light scattered from three alkali halide crystals: KCl, RbCl, and KI. By suitable orientation of the crystal axes relative to the incident beam we have obtained the frequency and the velocity of thermally excited phonons of $\sim 3000 \text{ \AA}$ wavelength in longitudinal and "mixed" acoustic phonon branches as a function of the direction of propagation in the $[110]$ plane. From these data we have determined for each crystal, entirely in the absence of acoustic excitation, the elastic constants C_{11} , C_{12} , and C_{44} for microwave (8–15 kMc/sec) sound waves with an accuracy from 0.25% to 4%. The elastic constants so determined are in very good agreement with investigations made in the ultrasonic region using externally generated sound waves of frequency $\sim 10 \text{ Mc/sec}$. This agreement indicates the absence of dispersion in the sound-wave velocity over three orders of magnitude change in the sound-wave frequency. We also present the theory for the scattering of light from thermally excited sound waves in a cubic crystal. This theory predicts the intensity, polarization, and spectral distribution of the scattered light as a function of the incident and scattered directions in the crystal. By treating the phonons quantum-mechanically at temperatures comparable to the scattering phonon frequency, we have also obtained expressions for the temperature dependence of the scattering valid at very low temperature. The theory is in quite good agreement with our measurements of the relative intensity of the scattering from phonons in the longitudinal and "mixed" acoustic modes.

I. INTRODUCTION

IF a beam of light passes through a solid or a liquid, a small fraction of the incident light will be scattered in all directions by thermal fluctuations in the dielectric constant of the medium. To be more precise, the light scattered an angle θ away from the forward direction results from a Bragg "reflection" off a thermal fluctuation whose wavelength (λ_f) is related to the wavelength of light in the medium (λ_0/n) by the Bragg condition:

$$(\lambda_0/n) = 2\lambda_f \sin(\theta/2),$$

where n is the index of refraction of the medium. From this condition we see that the wavelength of the scattering fluctuation ranges from one-half the wavelength of light in the medium for backward scattering to ($\lambda_0/n\theta$) near the forward direction.

The spectrum of the scattered light is determined by the time dependence of the fluctuations in the dielectric constant. Nonpropagating fluctuations produce scattered radiation whose central frequency is equal to that of the incident radiation. The frequency width of this "quasi-elastic" scattering is determined by the decay rate of the scattering fluctuation. On the other hand, suppose the fluctuation having wavelength λ_f propagates with a velocity $\pm V(\lambda_f)$ as do thermally excited sound waves. Under these conditions the light scattered from this fluctuation will suffer a Doppler shift on "reflection" and the light will contain a doublet called a Brillouin doublet^{1,2} at the frequencies $\nu_0 \pm \Delta\nu$, where

$$(\Delta\nu/\nu_0) = 2(V/c)n \sin(\theta/2),$$

and where ν_0 is the frequency of the incident light wave and c is the velocity of light in vacuo. This formula, first obtained by Brillouin,^{1,2} shows that the spectrum of the scattered light can provide the velocity of thermally excited sound waves whose wavelength is of the same size as the wavelength of light. Such sound waves have frequencies of the order of 3–10 kMc/sec in liquids and 10–50 kMc/sec in solids. The linewidth of the Brillouin doublets gives the lifetime of the scattering sound wave. In essence, then, the method of "Brillouin scattering" is to use heat to generate sound waves and light to detect the velocity and lifetimes of these waves.

This method of experimentation has become particularly useful since the development of optical masers whose high spectral purity, power, and directivity make them ideal light sources in Brillouin scattering experiments.^{3,4}

Long before the invention of these light sources the subject of light scattering had undergone a rich theoretical and experimental development. Following the appearance of Maxwell's equations, Lord Rayleigh calculated⁵ the scattering of light produced by a dielectric sphere with dimensions small compared to the wavelength of light and obtained the celebrated result that the intensity of the scattering varies as the reciprocal fourth power of the wavelength of the exciting light. He applied these results to the scattering of sunlight by molecules in the atmosphere, treating each of these as radiating independently of its neighboring molecule. No account was taken of the phase relations between different scatterers. On the basis of his analysis,

* This work was supported by the Advanced Research Projects Agency, under Contract No. SD 90.

† Now at Department of Physics, The Catholic University of America, Washington, D. C.

¹ L. Brillouin, *Compt. Rend.* **158**, 1331 (1914).

² L. Brillouin, *Ann. Phys. (Paris)* **17**, 88 (1922).

³ G. Benedek, J. B. Lastovka, K. Fritsch, and T. Greytak, *J. Opt. Soc. Am.* **54**, 1284 (1964).

⁴ R. Y. Chiao and B. P. Stoicheff, *J. Opt. Soc. Am.* **54**, 1286 (1964).

⁵ Lord Rayleigh, *Phil. Mag.* **41**, 107 (1871); **41**, 274 (1871); **41**, 447 (1871); **47**, 375 (1899).

Lord Rayleigh was able to explain the distribution of color in skylight and estimate Avogadro's number from the attenuation of sunlight as it passed through the atmosphere.

The theory of light scattering was extended to continuous media by Von Smoluchowski⁶ and Einstein,⁷ who explained the phenomenon of critical opalescence: the enormous increase in the scattering of light which takes place near the gas-liquid critical point. Einstein treated the fluid as a continuous medium whose homogeneity was disturbed by thermal fluctuations of the density. He decomposed these fluctuations into their Fourier components and obtained essentially the Bragg reflection conditions mentioned above, but this result appeared in the form of the Laue equations. Einstein evaluated the amplitude of the density fluctuations and showed that they grew very large because the work required to produce them grows very small as one approaches the critical point, where the bulk modulus is zero.

To obtain the spectrum of the scattered light it was necessary to know the time dependence of the density fluctuations. This time dependence was provided by Debye's⁸ theory of specific heat, which identified the thermal content of a body with the excitation of sound waves. Brillouin^{1,2} combined the Bragg reflection condition with the motion of the sound waves and predicted the appearance of doublets in the spectrum of the scattered light. As the wavelength of the incident radiation grows shorter and shorter, the Brillouin scattering goes over smoothly into the thermal diffuse scattering of x rays⁹ and coherent inelastic scattering of neutrons.¹⁰ The Brillouin doublets were first found by Gross¹¹ and later confirmed by others.¹²

Stimulated by Brillouin's theory and Gross' observation, Debye and Sears¹³ coupled an acoustic transducer into a liquid column to set up a pattern of standing waves. This density grating acted to produce diffraction of a light beam which was sent through the column. By observation of the diffraction pattern, and a knowledge of the transducer frequency, this type of experimentation, which is quite different from the spectroscopic study involved in Brillouin scattering, became¹⁴ a very useful method¹⁵ for the study of the velocity of sound

waves whose frequencies were low enough to be generated by acoustic transducers.

From the very beginning, workers investigating the Brillouin spectrum found, in addition to the Brillouin components, a central or unshifted component in the spectrum of the scattered light. This component persisted even after removal of all foreign impurities suspended in the medium.

Landau and Placzek^{16,17} proposed that this quasi-elastic scattering was produced by nonpropagating density fluctuations, or more properly by isobaric entropy fluctuations, and they calculated the intensity and spectral distribution of this component. Both the Brillouin and the Landau-Placzek theories have been cast in a more modern form^{18,19} which relates the spectrum of the scattered light to the space-time correlation functions for the density and temperature fluctuations.

Within the limits set by the spectral distribution and intensity of conventional light sources, the Brillouin spectrum has been studied both in liquids^{20,21} and in solids.²² The review of Fabelinskii²⁰ is particularly valuable. It includes an account of the early independent theoretical and experimental contributions made to this field by Mandel'shtam and Landsberg.

With the aid of laser light sources and high-resolution interference spectroscopy it has now become possible to measure,^{4,23-25} for the first time, lifetimes of the thermally excited microwave phonons, and to determine as well their velocity with a precision ($\sim 0.1\%$) one order of magnitude higher than has previously been possible. Furthermore, very recent developments²⁶⁻³⁰ in electronic light-beating techniques, which are based on the monochromaticity of the laser light, permit a study of the spectrum of the scattered light with a resolving power many orders of magnitude greater than can be achieved with optical methods.

¹⁶ L. Landau and G. Placzek, *Physik Z. Sowjetunion* **5**, 172 (1934).

¹⁷ L. Landau and E. M. Lifshitz, *Electrodynamics of Continuous Media* (Addison-Wesley Publishing Company, Inc., Reading, Massachusetts, 1960), pp. 393 ff.

¹⁸ R. Pecora, *J. Chem. Phys.* **40**, 1604 (1964).

¹⁹ R. D. Mountain, *Rev. Mod. Phys.* **38**, 205 (1966).

²⁰ I. Fabelinskii, *Usp. Fiz. Nauk* **63**, 355 (1957).

²¹ D. H. Rank, E. R. Shull, and D. W. Axford, *Nature* **164**, 67 (1949).

²² R. S. Krishnan, *Proc. Indian Acad. Sci.* **A41**, 91 (1955).

²³ D. I. Mash, V. S. Starunov, and I. Fabelinskii, *Zh. Eksperim. i Teor. Fiz.* **47**, 783 (1964) [English transl.: *Soviet Phys.—JETP* **20**, 523 (1965)].

²⁴ R. Y. Chiao and P. Fleury, *Physics of Quantum Electronics*, edited by P. Kelley, B. Lax, and P. E. Tannenwald (McGraw-Hill Book Publishers, Inc., New York, 1966).

²⁵ G. Benedek and T. Greytak, *Proc. IEEE* **53**, 1623 (1965).

²⁶ H. Z. Cummins, N. Knable, and Y. Yeh, *Phys. Rev. Letters* **12**, 150 (1964).

²⁷ S. S. Alpert, Y. Yeh, and E. Lipworth, *Phys. Rev. Letters* **14**, 486 (1965).

²⁸ D. A. Jennings and H. Takuma, *Appl. Phys. Letters* **5**, 241 (1964).

²⁹ J. B. Lastovka and G. B. Benedek, *Physics of Quantum Electronics*, edited by P. Kelley, B. Lax, and P. E. Tannenwald (McGraw-Hill Book Publishers, Inc., New York, 1966).

³⁰ N. C. Ford, Jr., and G. B. Benedek, *Phys. Rev. Letters* **15**, 694 (1965).

⁶ M. Von Smoluchowski, *Ann. Physik* **25**, 205 (1908).

⁷ A. Einstein, *Ann. Physik* **38**, 1275 (1910).

⁸ P. Debye, *Ann. Physik* **39**, 789 (1912).

⁹ R. W. James, *The Optical Principles of the Diffraction of X-Rays* (G. Bell and Sons, Ltd., London, 1958).

¹⁰ B. N. Brockhouse and A. T. Stewart, *Rev. Mod. Phys.* **30**, 236 (1958).

¹¹ E. Gross, *Nature*, **126**, 201 (1930); **126**, 400 (1930); **126**, 603 (1930); **129**, 722 (1932).

¹² E. H. L. Meyer and W. Ramm, *Physik. Z.* **33**, 270 (1932); **35**, 111, 756 (1934).

¹³ P. Debye and F. W. Sears, *Proc. Natl. Acad. Sci.* **18**, 409 (1932).

¹⁴ C. V. Raman and N. Nath, *Proc. Indian Acad. Sci.* **A2**, 406 (1935); **A2**, 413 (1935); **A3**, 75 (1936); **A3**, 119 (1936); **A3**, 459 (1936).

¹⁵ L. Bergmann, *Ultrasonics and their Scientific and Technical Applications* (John Wiley & Sons, Inc., New York, 1938).

In the present paper we present the results of a study^{31,32} of the Brillouin spectrum of light scattered from three alkali halide crystals, KI, KCl, and RbCl, using a helium-neon laser as a light source and a grating spectrograph. The spectrum was studied as a function of the angle between the crystal axes and the direction of the incident beam. This permits a measurement of the velocity of sound waves as a function of their direction in the crystal. In particular we have measured the velocity of sound waves in the longitudinal and "transverse" acoustic branches as a function of direction in the [110] crystal planes. The wavelength of sound studied was ~ 3000 Å, and the frequency of the longitudinal waves was ~ 10 kMc/sec while the "transverse" branch phonon frequencies were ~ 6 kMc/sec. From these data we have obtained with a precision between 0.25% and 4% the microwave elastic constants for these three crystals. We also present a calculation of the intensity, polarization, and spectral distribution of the scattered light along with the quantum-mechanical modifications required for application at very low temperatures. The predictions of this calculation are in good agreement with our measurements of the relative intensity of the scattering from "transverse" and longitudinal modes.

II. THEORY

We now present a classical calculation of the intensity and the spectrum of light scattered from thermal fluctuations in liquids and solids. At the outset it is important to recognize that these media contain about 10^9 atoms in a region as small as the cube of the light wavelength. Hence for dimensions of this order a liquid or solid may be regarded as a continuum. A light wave passing through such a medium produces an oscillating dipole moment per unit volume or polarization $\mathbf{P}(\mathbf{r}, t)$ at each point \mathbf{r} . The oscillating moments in turn radiate or scatter electromagnetic energy in all directions. The electric field $d\mathbf{E}'$ scattered to the field point \mathbf{R} by the oscillating polarization within a volume $|d\mathbf{r}| \ll \lambda^3$ is

$$d\mathbf{E}'(\mathbf{R}, t) = \left[\frac{\mathbf{1}_{\mathbf{R}-\mathbf{r}} \times (\mathbf{1}_{\mathbf{R}-\mathbf{r}} \times \partial^2 \mathbf{P}(\mathbf{r}, t') / \partial t'^2)}{c^2 |\mathbf{R}-\mathbf{r}|} |d\mathbf{r}| \right]_{t'=t-|\mathbf{R}-\mathbf{r}|/c_m} \quad (1)$$

The vectors \mathbf{R} , \mathbf{r} and the unit vectors $\mathbf{1}_{\mathbf{k}}$ and $\mathbf{1}_{\mathbf{R}-\mathbf{r}}$ are shown in Fig. 1. For simplicity we have taken the field point \mathbf{R} within the medium. If it is outside the medium one may find the field there by obtaining the scattered field inside the medium and then using the laws of refraction and reflection at the boundaries. In Eq. (1), t' is the retarded time $t - |\mathbf{R}-\mathbf{r}|/c_m$, calculated using as velocity the speed of light inside the medium (c_m) rather than that in a vacuum (c).

³¹ K. Fritsch, M.S. thesis, M.I.T., 1965 (unpublished).

³² K. Fritsch and G. Benedek, Bull. Am. Phys. Soc. **10**, 109 (1965).

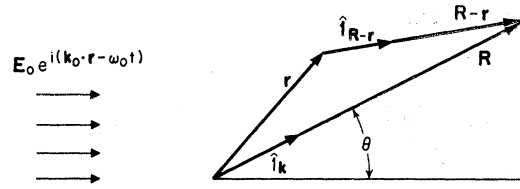


FIG. 1. Diagram showing the relationship between the source point \mathbf{r} , the field point \mathbf{R} , the incident wave vector \mathbf{k}_0 , and the scattering angle θ .

For low-intensity incident radiation, the local polarization is linearly proportional to the electric field, the proportionality factor being the tensor polarizability α . In analyzing the origin of the scattering it is convenient to decompose α into its time average part $\langle \alpha \rangle$ plus the time-space fluctuations $\delta\alpha(\mathbf{r}, t)$ produced by the thermal fluctuations in the medium. In liquids and in cubic crystals the time average polarizability $\langle \alpha \rangle$ is a scalar times the unity tensor, and the index of refraction n is independent of the direction of propagation. However, the thermal fluctuations in a crystal cause off-diagonal components to appear in the polarizability tensor, so that we must regard $\delta\alpha$ as being a tensor whose elements fluctuate in time. Writing then the electric field of the incident wave within the medium as

$$\mathbf{E}(\mathbf{r}, t) = \mathbf{E}_0 e^{i(\mathbf{k}_0 \cdot \mathbf{r} - \omega_0 t)}, \quad (2)$$

where $k_0 = n\omega_0/c$ is the wave vector of the light wave, we find that the polarization at each point in the medium is

$$\mathbf{P}(\mathbf{r}, t) = (\langle \alpha \rangle + \delta\alpha(\mathbf{r}, t)) \cdot \mathbf{E}_0 e^{i(\mathbf{k}_0 \cdot \mathbf{r} - \omega_0 t)}. \quad (3)$$

To evaluate the second derivative of \mathbf{P} as required by Eq. (1), we must realize that the characteristic frequencies for thermal fluctuations are small ($\lesssim 10^{12}$ cps) compared to the light frequency in the optical region ($\sim 5 \times 10^{14}$ cps). We may therefore regard $\delta\alpha$ as a very weak function of the time and write

$$\partial^2 \mathbf{P}(\mathbf{r}, t) / \partial t'^2 \cong -\omega_0^2 \mathbf{P}(\mathbf{r}, t). \quad (4)$$

On substituting Eqs. (3) and (4) into (1) and carrying out the integration over the illuminated volume V at the retarded time t' , we find that if $\mathbf{R} \gg \mathbf{r}$,

$$\mathbf{E}'(\mathbf{R}, t) = -\left(\frac{\omega_0}{c}\right)^2 \frac{e^{i(\mathbf{k}_0' \cdot \mathbf{R} - \omega_0 t)}}{R} \mathbf{1}_{\mathbf{k}} \times \left[\mathbf{1}_{\mathbf{k}} \times \int_V (\langle \alpha \rangle + \delta\alpha(\mathbf{r}, t')) \cdot \mathbf{E}_0 e^{i(\mathbf{k}_0 - \mathbf{k}_0') \cdot \mathbf{r}} |d\mathbf{r}| \right], \quad (5)$$

where we have used the facts that if $\mathbf{R} \gg \mathbf{r}$

$$\mathbf{1}_{\mathbf{R}-\mathbf{r}} \cong \mathbf{1}_{\mathbf{k}};$$

$$\frac{n\omega_0}{c} |\mathbf{R}-\mathbf{r}| \cong \frac{n\omega_0}{c} \mathbf{1}_{\mathbf{k}} \cdot (\mathbf{R}-\mathbf{r});$$

$$\mathbf{k}_0' \cong n\omega_0 \mathbf{1}_{\mathbf{k}} / c;$$

and in the denominator we have used

$$|\mathbf{R}-\mathbf{r}| \approx R.$$

The integral in Eq. (5) represents the superposition of phases of waves scattered from each illuminated point in the medium. In the absence of the fluctuations ($\delta\alpha$) this superposition leads to a complete cancellation of the scattered waves. The contribution to the integral from the $\langle\alpha\rangle$ term is zero except in the forward direction. Scattering out of the incident direction results entirely from fluctuations in the polarizability.

We may now ask: Of all the fluctuations, which in particular are responsible for the scattering of light into a particular direction? This can be answered by analyzing the fluctuations into their spatial Fourier components:

$$\delta\alpha(\mathbf{r},t') = \frac{1}{(2\pi)^{3/2}} \sum_{\mu} \int |d\mathbf{q}| \delta\alpha^{\mu}(\mathbf{q}) e^{i[\mathbf{q}\cdot\mathbf{r} \mp \omega_{\mu}(\mathbf{q})t']}. \quad (6)$$

In this decomposition $2\pi/|\mathbf{q}|$ is the wavelength of the fluctuation, $\omega_{\mu}(\mathbf{q})$ is the frequency of the fluctuation corresponding to this wavelength. The index μ denotes the possibility of a number of branches in the dispersion relation connecting \mathbf{q} and ω . In general, $\omega_{\mu}(\mathbf{q})$ can be complex to include a description of the damping of the fluctuations.³³ $\omega_{\mu}(\mathbf{q})$ is double valued with (\pm) to account for the degeneracy in the dispersion relation for positive and negative running waves. We now can put Eq. (6) into Eq. (5), being careful to include the effect of time retardation in $\delta\alpha$. This gives

$$\begin{aligned} \mathbf{E}'(\mathbf{R},t) = & -\left(\frac{\omega_0}{c}\right)^2 \sum_{\mu} \mathbf{1}_k \\ & \times \left[\mathbf{1}_k \times \int |d\mathbf{q}| (\delta\alpha^{\mu}(\mathbf{q}) \cdot \mathbf{E}_0) \frac{e^{i[\mathbf{k}\cdot\mathbf{R} - [\omega_0 \pm \omega_{\mu}(\mathbf{q})]t]}}{R} \right] \\ & \times \frac{1}{(2\pi)^{3/2}} \int |d\mathbf{r}| e^{i(\mathbf{k}_0 - \mathbf{k} + \mathbf{q})\cdot\mathbf{r}}, \quad (7) \end{aligned}$$

where

$$\mathbf{k} = (n/c)(\omega_0 \pm \omega_{\mu}(\mathbf{q}))\mathbf{1}_k = \mathbf{k}(\mathbf{q}). \quad (8)$$

The final integral in Eq. (7) is a delta function provided that the illuminated region is very large compared to the wavelength of light. In this case,

$$\int e^{i(\mathbf{k}_0 - \mathbf{k} + \mathbf{q})\cdot\mathbf{r}} |d\mathbf{r}| = (2\pi)^3 \delta[\mathbf{q} - (\mathbf{k}(\mathbf{q}) - \mathbf{k}_0)]. \quad (9)$$

Thus the wave vector of the fluctuation which produces the scattering in the direction $\mathbf{1}_k$ is that which satisfies the implicit equation

$$\mathbf{q} = \mathbf{k}(\mathbf{q}) - \mathbf{k}_0 \equiv \mathbf{K}. \quad (10)$$

³³ For the quasi-elastic or central component in the scattering $\omega_{\mu}(\mathbf{q})$ is purely imaginary.

The solution of this equation is denoted by \mathbf{K} and is called the scattering vector. Equation (10) for \mathbf{K} can be interpreted physically in two equivalent ways. In photon terminology it represents the conservation of momentum between the incident photon \mathbf{k}_0 , the scattered photon \mathbf{k} , and the scattering fluctuation \mathbf{K} . Here we must remember from Eq. (8) that the wavelength of the scattered light can be different from that of the incident light because the scattering fluctuation can exchange a quantum of energy $\pm\hbar\omega_{\mu}(\mathbf{K})$ with the incident photon. In classical terms, Eq. (10) represents the fact that a spatially periodic fluctuation can modulate the polarizability and hence the phase of waves scattered from each point in such a way as to exactly cancel out the phase factor $e^{i(\mathbf{k}-\mathbf{k}_0)\cdot\mathbf{r}}$ produced by the combined effect of the spatial variation of the incident wave and the time retardation. As a result of this cancellation the radiation from each point in the medium can add constructively at the field point. In this classical description, Eq. (10) corresponds to a Bragg reflection of the light waves off the wave fronts of the fluctuations. Substituting Eqs. (10) and (9) into (7) and replacing $\delta\alpha$ by $\delta\epsilon/4\pi$, where $\delta\epsilon$ is the fluctuation in the dielectric constant tensor, we find on relabeling $\mathbf{E}'(\mathbf{R},t) = \mathbf{E}'(\mathbf{K},t)$ (i.e., we emphasize the dependence of the scattered field on the *direction* of scattering),

$$\begin{aligned} \mathbf{E}'(\mathbf{K},t) = & -\left(\frac{\omega_0}{c}\right)^2 \frac{(2\pi)^{3/2}}{4\pi R} \sum_{\mu} e^{i[\mathbf{k}\cdot\mathbf{R} - [\omega_0 \pm \omega_{\mu}(\mathbf{K})]t]} \\ & \mathbf{1}_k \times [\mathbf{1}_k \times (\delta\epsilon^{\mu}(\mathbf{K}) \cdot \mathbf{E}_0)]. \quad (11) \end{aligned}$$

The amplitude of the scattering from each branch is proportional to that spatial Fourier component of the fluctuation in ϵ which has wave vector \mathbf{K} . The frequency of the scattered wave (ω') is shifted from that of the incident wave ω_0 by the amount $\pm\omega_{\mu}(\mathbf{K})$, i.e.,

$$\omega' = \omega_0 \pm \omega_{\mu}(\mathbf{K}). \quad (12)$$

The spectrum of the scattered light contains sets of doublets located symmetrically around the incident light frequency. In quantum-mechanical language these doublets represent the exchange of a quantum $\pm\hbar\omega(\mathbf{K})$ between the photon and the fluctuation. Classically, the frequency change of the scattered light follows from the picture of its origin as a Bragg reflection, provided that we include the fact that the wave fronts of the fluctuation move with the phase velocity $[\pm\omega_{\mu}(\mathbf{K})/\mathbf{K}]$. Because of this, the incident light wave suffers a Doppler shift which is exactly equal to that given in Eq. (12).

To determine the spacing between the doublets, and the scattering vectors \mathbf{K} involved, it is necessary to identify in greater detail the nature of the microscopic fluctuations. One source of these is to be found in the lattice vibrations in liquids and solids. These traveling waves produce fluctuations with wave vectors \mathbf{q} in the

range $0 < |\mathbf{q}| < \pi/a_0$, where a_0 is a distance of the order of the interatomic spacing. The corresponding dispersion relations $[\omega_\mu(\mathbf{q})]$ consist, in general, of optical and acoustical branches. If we solve Eq. (10) using Eq. (8) for either of these branches, we find at once that the scattering vectors \mathbf{K} fall in the range $0 < |\mathbf{K}| < (4\pi/\lambda)$, where λ is the wavelength of light in the medium. Hence, the lattice vibrations do indeed contain waves whose wavelengths satisfy the momentum conservation condition. However, since visible light has $\lambda \sim 10^3 a_0$, the scattering is produced by phonons whose wave vectors span the region in reciprocal space between the origin and points one-thousandth of the distance to the edge of the Brillouin zone. While these points are far from the zone edge, they represent regions of the phonon spectrum which are far beyond the ultrasonic region.

The scattering which comes from the optical branches in solids is called vibrational Raman scattering. The frequency shift involved is $\Delta\omega \sim 2\pi \times 10^{12}/\text{sec}$ and this shift depends only weakly on the scattering vector \mathbf{K} because of the flatness of the $\omega(\mathbf{K})$ curves in the optical branches. A particular optical branch will be Raman active for a given \mathbf{K} provided that it produces a fluctuation in the dielectric constant with that wave vector. Scattering from the acoustic branches is known as Brillouin scattering,^{1,2} and involves a frequency shift which is 10^3 to 10^4 times smaller than that of the Raman effect. This frequency shift, $[\pm\omega_\mu(\mathbf{K})]$, reflects directly the dispersion relation for phonons in the acoustic branches.

The angular dependence of the Brillouin doublet spacing is computed as follows: Let the light be scattered a direction θ away from the incident beam. The scattering vector \mathbf{K} is calculated to a high degree of accuracy by neglecting the change in wavelength of the scattered light in Eqs. (10) and (9). Under this approximation \mathbf{k} and \mathbf{k}_0 have the same length and \mathbf{K} simply connects them. The direction of \mathbf{K} is perpendicular to the line bisecting the angle θ and has the length

$$K \cong 2k_0 \sin(\theta/2) = (2n\omega_0/c) \sin(\theta/2). \quad (13)$$

The corresponding shift $(\omega' - \omega_0)$ in frequency of the scattered light is determined by the acoustic dispersion relations:

$$\omega_\mu(\mathbf{K}) = V(\omega_\mu, \mathbf{1}_K) K. \quad (14)$$

Here we take explicit note of the fact that the phase velocity (V) can be a function of the frequency and the direction of the sound wave. Combining Eqs. (14) and (13) we obtain the result first found by Brillouin,^{1,2} viz.,

$$\frac{\omega' - \omega_0}{\omega_0} = \pm \frac{\omega_\mu(\mathbf{K})}{\omega_0} = \pm \frac{2nV(\omega_\mu, \mathbf{1}_K)}{c} \sin(\theta/2). \quad (15)$$

In liquids the velocity is independent of the direction of propagation and only a longitudinal acoustic branch exists, i.e., $V = V(\omega)$. As the scattering angle θ increases,

the scattering phonon, and hence the shift $\omega' - \omega_0$, ranges from 0 in the forward direction to $\omega \sim 2 \times 10^{-5} \omega_0$ for backward scattering. For visible light this corresponds to a phonon frequency of $\sim 10 \times 10^9$ cps. Hence by studying the angular dependence of the splitting of the "Brillouin doublets" we may obtain the sound velocity as a function of frequency up to about 10 kMc in liquids.

The Brillouin spectrum of light scattered from a solid differs from that of a liquid. In the solid, the length and direction of the scattering vector \mathbf{K} is, as before, fixed to a high degree of approximation by n and the angle θ [Eq. (13)] between incident and scattered beam. However, in the solid the acoustic phonons contain three separate branches: there are in general three different frequency sound waves, each with the same wave vector \mathbf{K} . The Brillouin spectrum, therefore, contains, in general, three sets of doublets. Furthermore, in the solid, one can bring different crystal directions into coincidence with the vector \mathbf{K} without in any way altering the scattering angle θ . Hence, one may obtain from the Brillouin spectra the frequency and the phase velocity of sound waves with wave vector $|\mathbf{K}| = 2(n\omega_0/c) \sin\theta/2$ as a function of direction in the crystal. In the present experiments we have carried out this procedure for the three cubic crystals, KCl, KI, and RbCl. We fixed the scattering angle θ at 90° and thereby selected the wavelength of phonons to be investigated ($\sim 3000 \text{ \AA}$). The crystal axes were rotated so that the scattering from phonons anywhere in the $[110]$ plane could be studied. From the observed splitting of the Brillouin components produced by phonons in the "longitudinal" and "transverse" branches we obtained the angular dependence of the phase velocity and the frequency for sound waves with the prechosen wavelength. With this information we have determined for the first time the elastic constants of these crystals in the 6–15 kMc/sec region. To investigate curvature in the $\omega(\mathbf{K})$ curves one can measure the phase velocity as a function of wavelength simply by altering the scattering angle θ .

If we include the change in wavelength of the scattered light in computing the scattering vector \mathbf{K} from Eqs. (10) and (8), it can be shown that there is a slight asymmetry in the placement of the Brillouin doublets around the unshifted frequency ω_0 . The high-frequency line is shifted an amount $\delta\omega_\mu$ farther away from ω_0 , while the low-frequency line is shifted toward ω_0 by $\delta\omega_\mu$. In fact it is easy to show that $(\delta\omega_\mu/\omega_\mu) = \frac{1}{2}(\omega_\mu/\omega_0)$. This is approximately 10^{-6} to 10^{-5} for most liquids and solids. This effect is too small to be detected in the present experiments.

The analysis presented above has centered on the information contained in the location of the centers of the Brillouin doublets. We now calculate the intensity and the spectral distribution of the scattered radiation. Both these quantities are determined by the autocorrelation function for the scattered electric field,

viz.,

$$\langle \mathbf{E}'(\mathbf{K}, t+\tau) \cdot \mathbf{E}^*(\mathbf{K}, t) \rangle \\ \equiv \lim_{T \rightarrow \infty} \frac{1}{2T} \int_{-T}^T \mathbf{E}'(\mathbf{K}, t+\tau) \cdot \mathbf{E}^*(\mathbf{K}, t) dt. \quad (16)$$

The total power $dP'[(\mathbf{K}, \mathbf{R})]$ in all frequencies scattered into a solid angle $d\Omega$ at the field point \mathbf{R} is proportional to the mean squared field strength,

$$dP'(\mathbf{K}, \mathbf{R}) = \frac{c}{8\pi} \langle |\mathbf{E}'(\mathbf{K}, t)|^2 \rangle R^2 d\Omega. \quad (17)$$

If we define the spectral density function $S(\mathbf{K}, \omega')$ as

$$S(\mathbf{K}, \omega') = \frac{1}{2\pi} \frac{\int_{-\infty}^{\infty} \langle \mathbf{E}'(\mathbf{K}, t+\tau) \cdot \mathbf{E}^*(\mathbf{K}, t) \rangle e^{i\omega'\tau} d\tau}{\langle |\mathbf{E}'(\mathbf{K}, t)|^2 \rangle}, \quad (18)$$

which is normalized in such a way that

$$\int_{-\infty}^{\infty} d\omega' S(\mathbf{K}, \omega') = 1, \quad (19)$$

then the power scattered into $d\Omega$ which lies in a frequency interval between ω' and $\omega'+d\omega'$, $[dP'(\mathbf{K}, \omega')d\omega']$ is given by

$$dP'(\mathbf{K}, \omega')d\omega' = (dP'(\mathbf{K}))S(\mathbf{K}, \omega')d\omega'. \quad (20)$$

In determining the form of the correlation function for the scattered field, it is convenient to reabsorb into $\delta\mathbf{e}^\mu(\mathbf{K})$ its corresponding time dependence. Writing then

$$\delta\mathbf{e}^\mu(\mathbf{K}, t) = \delta\mathbf{e}^\mu(\mathbf{K}) e^{-i\omega_\mu(\mathbf{K})t}, \quad (21)$$

Eq. (11) for the scattered field becomes

$$\mathbf{E}'(\mathbf{K}, t) = -\left(\frac{\omega_0}{c}\right)^2 \frac{(2\pi)^{3/2}}{4\pi R} \sum_{\mu} e^{i(\mathbf{k} \cdot \mathbf{R} - \omega_0 t)} \mathbf{1}_{\mathbf{k}} \\ \times [\mathbf{1}_{\mathbf{k}} \times (\delta\mathbf{e}^\mu(\mathbf{K}, t) \cdot \mathbf{E}_0)]. \quad (22)$$

This equation shows that the correlation function for the scattered field is determined by the fluctuations in the dielectric constant tensor. A fluctuation $\delta\mathbf{e}(\mathbf{K}, t)$ produces a corresponding fluctuation in the electric displacement vector $\delta\mathbf{D}(\mathbf{K}, t) = \delta\mathbf{e}(\mathbf{K}, t) \cdot \mathbf{E}_0$. The double cross product preceding this simply indicates that in the light-scattering experiments we observe the component of the fluctuations in $\delta\mathbf{D}(\mathbf{K}, t)$ which lie in a plane perpendicular to the direction of the scattered wave.

The fluctuations in the dielectric constant tensor components result from the fact that these components depend on the state of strain of the solid. The strains themselves fluctuate at each point because of the passage of thermally excited sound waves. In general,

for small strains, we may express the change in dielectric tensor component $\delta\epsilon_{ij}(\mathbf{r}, t)$ as a linear function of the elastic-strain components $e_{lm}(\mathbf{r}, t)$, viz.,

$$-\frac{\delta\epsilon_{ij}(\mathbf{r}, t)}{\epsilon_0^2} \equiv \sum_{l,m} p_{ijlm} e_{lm}(\mathbf{r}, t). \quad (23)$$

In a cubic crystal the coefficients p_{ijlm} , as defined above, are the Pockels elasto-optical constants.^{34,35} The strain components $e_{lm}(\mathbf{r}, t)$ are related to the elastic displacements $[u(r, t)]$ in the medium by

$$e_{lm}(\mathbf{r}, t) = \frac{1}{2} \left(\frac{\partial u_l(\mathbf{r}, t)}{\partial x_m} + \frac{\partial u_m(\mathbf{r}, t)}{\partial x_l} \right), \quad (24)$$

where l or m can take on the values 1, 2, or 3 and the x_1, x_2 , and x_3 represent the 3 coordinate axes relative to which the tensor components p_{ijlm} are defined. In a cubic crystal in which each cube axis has a fourfold symmetry, there are only three independent constants in the elasto-optical tensor and we may write Eq. (23) as

$$-\frac{\delta\epsilon_{ij}(\mathbf{r}, t)}{\epsilon_0^2} = p_{44} e_{ij}(\mathbf{r}, t) + (p_{11} - p_{12} - p_{44}) \delta_{ij} e_{ii}(\mathbf{r}, t) \\ + p_{12} \left(\sum_l e_{ll}(\mathbf{r}, t) \right) \delta_{ij}. \quad (25)$$

The elasto-optical coefficients p_{ij} in Eq. (25) are dimensionless quantities whose order of magnitude can be simply estimated. Consider for example the alteration of the optical dielectric-constant tensor produced by an adiabatic hydrostatic compression. In such a compression $e_{ij} = -\delta_{ij}(1/3)(\delta\rho/\rho)_s$, where ρ is the density of the solid and the subscript denotes a derivative at constant entropy. From Eq. (25) we see at once that the resulting alteration in the dielectric constant tensor is $\delta\epsilon_{ij} \equiv \delta_{ij} \delta\epsilon_0$, and that $\delta\epsilon_0$ is related to the p 's by

$$\left(\frac{p_{11} + 2p_{12}}{3} \right) = \frac{1}{\epsilon_0^2} \left(\frac{\delta\epsilon_0}{(\delta\rho/\rho)_s} \right) = \frac{1}{\epsilon_0} \left(\frac{\partial \ln \epsilon_0}{\partial \ln \rho} \right)_s. \quad (26)$$

Since $n^2 = \epsilon_0 \approx 3$, and since we may expect $(\partial \ln \epsilon_0 / \partial \ln \rho)_s \approx 1$, the magnitude of $(p_{11} + 2p_{12})/3$ is ~ 0.3 or of the order of unity.

It is also informative to examine the form of Eq. (25) for isotropic solids and for liquids. In the former case there are only two independent Pockels constants, p_{11} and p_{12} , and Eq. (23) takes Landau's form¹⁷

$$-\frac{\delta\epsilon_{ij}(\mathbf{r}, t)}{\epsilon_0^2} = (p_{11} - p_{12}) e_{ij}(\mathbf{r}, t) + p_{12} \left(\sum_l e_{ll}(\mathbf{r}, t) \right) \delta_{ij}. \quad (27)$$

In a liquid there is but one elasto-optical coefficient,

³⁴ J. F. Nye, *Physical Properties of Crystals*, Oxford (Clarendon Press, Oxford, England, 1957), pp. 243 ff.

³⁵ M. Born and K. Huang, *Dynamical Theory of Crystal Lattices* (Clarendon Press, Oxford, England, 1954), pp. 373 ff.

$p_{11}=p_{12}$ and the fluctuations in the dielectric constant tensor are just $\delta\epsilon_{ij}=\delta_{ij}\delta\epsilon_0$, where

$$\delta\epsilon_0(\mathbf{r},t)=-\epsilon_0^2 p_{11} \nabla \cdot \mathbf{u}(\mathbf{r},t)=p_{11}\epsilon_0^2(\delta\rho/\rho)_s, \quad (28)$$

where we have used $\nabla \cdot \mathbf{u} = -(\delta\rho/\rho)$ for sound waves in a liquid. In a liquid p_{11} is related very simply to the density dependence of ϵ_0 . In fact from (26) we see that in a liquid that $p_{11}=(1/\epsilon_0)(\partial \ln \epsilon_0/\partial \ln \rho)_s$, so that (28) takes the simple form

$$(\delta\epsilon_0(\mathbf{r},t))_s = \left(\frac{\partial \epsilon_0}{\partial \rho} \right)_s (\delta\rho)_s. \quad (29)$$

Having investigated the properties of the elastooptical tensor we return to the determination of $\delta\epsilon_{ij}(\mathbf{K},t)$, the fluctuation in the dielectric tensor components having wave vector \mathbf{K} . This quantity is given by

$$\delta\epsilon_{ij}(\mathbf{K},t) = \frac{1}{(2\pi)^{3/2}} \int |d\mathbf{r}| \delta\epsilon_{ij}(\mathbf{r},t) e^{-i\mathbf{K}\cdot\mathbf{r}}. \quad (30)$$

In the case of cubic crystals we must substitute Eq. (25) into (30). This yields an expression for $\delta\epsilon_{ij}(\mathbf{K},t)$ identical in form to (25) except that $e_{lm}(\mathbf{r},t)$ is replaced by its Fourier transform $e_{lm}(\mathbf{K},t)$, where

$$e_{lm}(\mathbf{K},t) = \frac{1}{(2\pi)^{3/2}} \int \frac{|d\mathbf{r}|}{2} \times \left(\frac{\partial u_l(\mathbf{r},t)}{\partial x_m} + \frac{\partial u_m(\mathbf{r},t)}{\partial x_l} \right) e^{-i\mathbf{K}\cdot\mathbf{r}}. \quad (31)$$

The sound waves produce a displacement at \mathbf{r} which is due to the superposition of waves with all possible wave vectors \mathbf{q} , i.e.,

$$u_l(\mathbf{r},t) = \frac{1}{(2\pi)^{3/2}} \int u_l(\mathbf{q},t) e^{i\mathbf{q}\cdot\mathbf{r}} d\mathbf{q}. \quad (32)$$

Substitution of Eq. (32) into Eq. (31) and integration over $|d\mathbf{r}|$ shows that the fluctuation $\delta\epsilon_{lm}(\mathbf{K},t)$ is produced solely by the strains of the sound waves which propagate with wave vector \mathbf{K} . There are only three such waves corresponding to the three possible polarizations of the wave. Denoting the polarization index by $\mu=1, 2, \text{ or } 3$ as in Eq. (22), we have

$$e_{lm}(\mathbf{K},t) = \frac{i}{2} (u_l^\mu(\mathbf{K},t) K_m + u_m^\mu(\mathbf{K},t) K_l). \quad (33)$$

$u_l^\mu(\mathbf{K},t)$ is the Fourier amplitude of the displacement vector along the l coordinate axis of the sound wave having wave vector \mathbf{K} and polarization μ . Using Eq. (33) we find that the substitution of Eq. (25) into Eq. (30) gives the following result for the fluctuation in the electric displacement vector $\delta\mathbf{D}(\mathbf{K},t)$ produced by the

sound waves in conjunction with E_0 :

$$\delta\mathbf{D}^\mu(\mathbf{K},t) \equiv \delta e^\mu(\mathbf{K},t) \cdot \mathbf{E}_0 = \frac{\epsilon_0^2}{i} u^\mu(\mathbf{K},t) K E_0 \zeta^\mu, \quad (34)$$

where K and E_0 are the magnitudes of K and E_0 , respectively.

$$\mathbf{u}^\mu(\mathbf{K},t) = \mathbf{u}'^\mu(\mathbf{K}) e^{\pm i\omega_\mu(\mathbf{K})t} \quad (35)$$

represents the amplitude and time dependence of the elastic displacement in the sound wave. ζ^μ is a vector whose magnitude is $0 < |\zeta| \lesssim 1$. Its value is given by

$$\zeta^\mu = \frac{p_{44}}{2} (\hat{\pi}^\mu \cdot \mathbf{1}_{\mathbf{K}} \cdot \mathbf{1}_{\mathbf{E}_0}) + (\hat{\pi}^\mu \cdot \mathbf{1}_{\mathbf{E}_0}) \mathbf{1}_{\mathbf{K}} + p_{12} (\hat{\pi}^\mu \cdot \mathbf{1}_{\mathbf{K}}) \mathbf{1}_{\mathbf{E}_0} + (p_{11} - p_{12} - p_{44}) \sum_{l=1}^3 \hat{\pi}^l (\mathbf{1}_{\mathbf{K}})_l (\mathbf{1}_{\mathbf{E}_0})_l \mathbf{1}_l, \quad (36)$$

where $\hat{\pi}^\mu$ is a unit vector in the direction of the polarization of the sound wave. The components of $\hat{\pi}^\mu$ along the cube axes are π^l , $l=1, 2, 3$. $\mathbf{1}_{\mathbf{K}}$ is a unit vector in the direction of propagation of the sound wave, with components $(\mathbf{1}_{\mathbf{K}})_l$ along the cube axes. $\mathbf{1}_{\mathbf{E}_0}$ is a unit vector along the direction of polarization of the incident light-wave. The components of this unit vector are $(\mathbf{1}_{\mathbf{E}_0})_l$ along the cube axes. $\mathbf{1}_l$ ($l=1, 2, \text{ or } 3$) are unit vectors along the cube axes. The direction and magnitude of ζ is determined by the relative directions of \mathbf{K} , \mathbf{E}_0 , and $\hat{\pi}^\mu$ and the magnitude of the p 's. We note that in general the electric displacement is in a different direction from that of the incident field \mathbf{E}_0 . As was mentioned before, we observe in the light-scattering experiments not ζ^μ , but the vector ξ^μ which is related to ζ^μ by

$$\xi^\mu = \mathbf{1}_{\mathbf{K}} \times (\mathbf{1}_{\mathbf{K}} \times \zeta^\mu). \quad (37)$$

This quantity is simply the component of ζ which lies in the plane perpendicular to \mathbf{k} . We shall presently give explicit expressions for ξ for those directions of $\mathbf{1}_{\mathbf{K}}$, $\mathbf{1}_{\mathbf{E}_0}$, and $\hat{\pi}^\mu$ which obtain in the present experiments.

We can now obtain expressions for the correlation functions for the scattered electric field using Eq. (22) and Eqs. (34)–(37). Remembering that sound waves belonging to different polarization branches are orthogonal to one another we have

$$\langle \mathbf{E}'(\mathbf{K},t+\tau) \cdot \mathbf{E}'^*(\mathbf{K},t) \rangle = \left(\frac{\omega_0}{c} \right)^4 \frac{(2\pi)^3 \epsilon_0^4}{(4\pi)^2 R^2} K^2 E_0^2 \times \sum_{\mu=1}^3 |\xi^\mu|^2 \langle \mathbf{u}^\mu(\mathbf{K},t+\tau) \cdot \mathbf{u}^{\mu*}(\mathbf{K},t) \rangle e^{-i\omega_0\tau}. \quad (38)$$

The correlation function for $\mathbf{u}^\mu(\mathbf{K},t)$ may be obtained by reasoning along the following lines. In Eq. (35) we broke the time dependence of the thermally excited sound-wave displacement $\mathbf{u}^\mu(\mathbf{K},t)$ into two parts: one being the rapid sound oscillation frequency, the other being much slower statistical fluctuations in the amplitude factor $u'^\mu(K,t)$. This amplitude factor is in fact a random variable. If we characterize the temporal

coherence of this variable by a correlation time $\tau_\mu(\mathbf{K})$ or a correlation rate $1/\Gamma_\mu(\mathbf{K})$ and presume that the correlation function for this amplitude dies away exponentially in time then it follows that

$$\begin{aligned} \langle \mathbf{u}^\mu(\mathbf{K}, t+\tau) \cdot \mathbf{u}^{\mu*}(\mathbf{K}, t) \rangle &= \langle \mathbf{u}'^\mu(\mathbf{K}, t+\tau) \mathbf{u}'^{\mu*}(\mathbf{K}, t) \rangle e^{\pm i\omega_\mu(\mathbf{K})\tau} \\ &= \langle |\mathbf{u}'^\mu(\mathbf{K}, t)|^2 \rangle e^{\pm i\omega_\mu(\mathbf{K})\tau} e^{-\Gamma_\mu(\mathbf{K})\tau}. \end{aligned} \quad (39)$$

We observe that $\Gamma_\mu(\mathbf{K})$ is the decay rate for the sound wave of wave vector \mathbf{K} . The mean squared amplitude of the sound wave can be related to the temperature as follows. The total vibrational energy of the solid is equal (by the equipartition theorem for harmonic oscillators) to twice the kinetic energy.

$$\langle E \rangle = 2\langle T \rangle = \left\langle \int |d\mathbf{r}| \rho |\dot{\mathbf{u}}(\mathbf{r}, t)|^2 \right\rangle, \quad (40)$$

where ρ is the density. The sound wave amplitude enters into the expression for the energy through the relation

$$\mathbf{u}(\mathbf{r}, t) = \frac{1}{(2\pi)^{3/2}} \sum_\mu \int |d\mathbf{q}| \mathbf{u}^\mu(\mathbf{q}) e^{i[\mathbf{q} \cdot \mathbf{r} \mp \omega_\mu(\mathbf{q})]t}. \quad (41)$$

Substituting this into Eq. (40) we find, keeping in mind that Eq. (41) indicates that for a single \mathbf{q} there are two sound waves moving in opposite directions

$$\langle E \rangle = 2 \sum_\mu \int |d\mathbf{q}| \rho \omega_\mu^2(\mathbf{q}) |\mathbf{u}^\mu(\mathbf{q})|^2. \quad (42)$$

From Eq. (42) we note that the Fourier amplitudes $\mathbf{u}(\mathbf{q})$ are the normal coordinates for the lattice vibrations. Denoting by $\langle E_\mu(\mathbf{q}) \rangle$ the thermal average of the energy for each normal mode, we note that the total

energy is simply equal to the sum over all the normal mode energies. Writing this sum as an integral over $|d\mathbf{q}|$ with the appropriate density of states we have that

$$\langle E \rangle = \sum_\mu \int \frac{V}{(2\pi)^3} |d\mathbf{q}| \langle E_\mu(\mathbf{q}) \rangle, \quad (43)$$

where V is the volume of the solid.

Comparing Eqs. (43) and (42) and using the fact that for $kT \gg \hbar\omega$ $\langle E_\mu(\mathbf{q}) \rangle = kT$ we find that

$$\langle |\mathbf{u}^\mu(\mathbf{K})|^2 \rangle = \frac{V}{(2\pi)^3} \frac{kT}{2\rho\omega_\mu^2(\mathbf{K})}. \quad (44)$$

Hence the correlation function for the scattered field becomes

$$\begin{aligned} \langle \mathbf{E}'(\mathbf{K}, t+\tau) \cdot \mathbf{E}^*(\mathbf{K}, t) \rangle &= E_0^2 \left(\frac{\omega_0}{c} \right)^4 \frac{\epsilon_0^4}{R^2} \frac{V}{(4\pi)^2} \frac{kT}{2\rho} \\ &\times \sum_{\mu=1}^3 |\xi^\mu|^2 \frac{K^2}{\omega_\mu^2(\mathbf{K})} e^{-i[\omega_0 \mp \omega_\mu(\mathbf{K})]\tau} (e^{-\Gamma_\mu(\mathbf{K})\tau}). \end{aligned} \quad (45)$$

It should be mentioned that the \mp notation in Eq. (45) indicates that a sum is to be taken over both the positive and negative running waves.

Now that this correlation function has been determined we find that the total power scattered into a solid angle $d\Omega$ is given by Eq. (17), where the auto-correlation function for the scattered field is

$$\langle |\mathbf{E}'(\mathbf{K}, t)|^2 \rangle = E_0^2 \left(\frac{\omega_0}{c} \right)^4 \frac{\epsilon_0^4}{R^2} \frac{V}{(4\pi)^2} \frac{kT}{\rho} \sum_{\mu=1}^3 \frac{|\xi^\mu|^2 K^2}{\omega_\mu^2(\mathbf{K})}. \quad (46)$$

This power is distributed over a spectrum whose density $S(\mathbf{K}, \omega')$ is given according to Eq. (18) by

$$S(\mathbf{K}, \omega') = \frac{\sum_{\mu=1}^3 \frac{|\xi^\mu|^2}{\omega_\mu^2(\mathbf{K})} \frac{1}{\pi} \left\{ \frac{\Gamma_\mu(\mathbf{K})}{(\omega' - [\omega_0 + \omega_\mu(\mathbf{K})])^2 + \Gamma_\mu^2(\mathbf{K})} + \frac{\Gamma_\mu(\mathbf{K})}{(\omega' - [\omega_0 - \omega_\mu(\mathbf{K})])^2 + \Gamma_\mu^2(\mathbf{K})} \right\}}{2 \sum_{\mu=1}^3 \frac{|\xi^\mu|^2}{\omega_\mu^2(\mathbf{K})}}. \quad (47)$$

Thus, as we have already realized previously, the spectrum of the scattered radiation consists in general of three pairs of doublets split around the incident frequency by the frequency $\omega_\mu(\mathbf{K})$ of the three sound waves having wave vector \mathbf{K} . The width of each of these spectral lines gives the sound wave lifetime $[1/\Gamma_\mu(\mathbf{K})]$. By changing the direction of observation and by rotating the crystal axes relative to the scattering direction one can study the dependence of the lifetime on the sound wavelength and on its direction of propagation in the crystal. Such an investigation requires of course that the spectral distribution in the incident laser beam be smaller than the spectral width of the scattered Brillouin components

and that the spectrometer have sufficient resolving power. Finally we note that the factors $|\xi^\mu|^2$ play the role of weighting factors which determine the relative intensities of each of the three doublets.

Equation (45) for the correlation function for the scattered field was derived under the assumption $\hbar\omega_\mu \ll kT$. Since the maximum sound wave frequencies which contribute to the scattering are about 50×10^9 cps, we expect that Eq. (45) will be valid provided that $T \gg 3^\circ\text{K}$. If the temperature falls into the 4°K region, however, Eq. (45) must be altered to take into account the quantum mechanical features of the lattice vibrations. We may obtain the correct quantum

mechanical results by making the following replacements in Eq. (39):

$$|\mathbf{u}(\mathbf{K})|^2 e^{i\omega_\mu(\mathbf{K})\tau} \rightarrow \langle |(n' | \mathbf{u}^{\mu+}(\mathbf{K}) | n)|^2 e^{i\omega_\mu(\mathbf{K})\tau} \rangle, \quad (48)$$

and

$$|\mathbf{u}(\mathbf{K})|^2 e^{-i\omega_\mu(\mathbf{K})\tau} \rightarrow \langle |(n' | \mathbf{u}^\mu(\mathbf{K}) | n)|^2 e^{-i\omega_\mu(\mathbf{K})\tau} \rangle. \quad (49)$$

That is, \mathbf{u} 's become, in the quantum mechanical case, the phonon creation and annihilation operators and one must evaluate the thermal average $\langle \rangle$ of the matrix elements of these operators. These averages are

$$\langle |(n' | \mathbf{u}^{\mu+}(\mathbf{K}) | n)|^2 \rangle = \frac{V}{(2\pi)^3} \frac{\hbar\omega_\mu(\mathbf{K})(\langle n_\mu(\mathbf{K}) \rangle + 1)}{2\rho\omega_\mu^2(\mathbf{K})}, \quad (50)$$

$$\langle |(n' | \mathbf{u}^\mu(\mathbf{K}) | n)|^2 \rangle = \frac{V}{(2\pi)^3} \frac{\hbar\omega_\mu(\mathbf{K})(\langle n_\mu(\mathbf{K}) \rangle)}{2\rho\omega_\mu^2(\mathbf{K})}, \quad (51)$$

where $\langle n_\mu(\mathbf{K}) \rangle$ is the mean occupation number of the phonons having wave vector \mathbf{K} and polarization index μ :

$$\langle n_\mu(\mathbf{K}) \rangle = (e^{\hbar\omega_\mu(\mathbf{K})/kT} - 1)^{-1}. \quad (52)$$

The correct form for Eq. (45) at all temperatures is

$$\begin{aligned} & \langle \mathbf{E}'(\mathbf{K}, t + \tau) \cdot \mathbf{E}''(\mathbf{K}, t) \rangle \\ &= E_0^2 \left(\frac{\omega_0}{c} \right)^4 \frac{\epsilon_0^4}{R^2} \frac{V}{(4\pi)^2} \frac{1}{2\rho} \sum_{\mu=1}^3 |\xi^\mu|^2 \frac{K^2 \hbar\omega_\mu(\mathbf{K})}{\omega_\mu^2(\mathbf{K})} \\ & \quad \times \left[\langle (n_\mu(\mathbf{K}) + 1) e^{-i[\omega_0 - \omega_\mu(\mathbf{K})]\tau} \right. \\ & \quad \left. + \langle n_\mu(\mathbf{K}) e^{-i[\omega_0 + \omega_\mu(\mathbf{K})]\tau} \right] e^{-\Gamma_\mu(\mathbf{K})\tau}. \quad (53) \end{aligned}$$

The power scattered into the solid angle $d\Omega$ is proportional [through Eq. (17)] to the value that Eq. (53) takes for $\tau=0$. We note that even at $T=0^\circ\text{K}$, where all the phonons are in the ground states, the zero-point motions still produce scattering. In fact, Eq. (53) shows that the scattering power at 0°K is equal to that obtained from the classical formula provided that we replace kT by the zero point energy $\hbar\omega/2$. The spectrum of the scattered light becomes asymmetrical as $kT \lesssim \hbar\omega_\mu(\mathbf{K})$, as can be seen by taking the time Fourier spectrum of the correlation function [Eq. (18)]. This gives the following form for the spectrum of scattered light:

$$\begin{aligned} S(\mathbf{K}, \omega) &= \left\{ \sum_{\mu=1}^3 \frac{|\xi^\mu|^2}{\omega_\mu^2(K)} \frac{\hbar\omega_\mu(\mathbf{K})\Gamma_\mu(\mathbf{K})}{\pi} \right\} \\ & \quad \times \left\{ \frac{\langle (n_\mu(\mathbf{K}) + 1) \rangle}{[\omega' - (\omega_0 - \omega_\mu(\mathbf{K}))]^2 + \Gamma_\mu^2(K)} \right. \\ & \quad \left. + \frac{\langle n_\mu(\mathbf{K}) \rangle}{[\omega' - (\omega_0 + \omega_\mu(\mathbf{K}))]^2 + \Gamma_\mu^2(K)} \right\} \\ & \quad \times \left\{ \sum_{\mu=1}^3 \frac{|\xi^\mu|^2}{\omega_\mu^2(K)} \hbar\omega_\mu(\mathbf{K})(2\langle n_\mu(\mathbf{K}) \rangle + 1) \right\}^{-1}. \quad (54) \end{aligned}$$

This shows that the spectrum of doublets becomes asymmetrical at low temperatures. As $T \rightarrow 0$, the amount of light in the low-frequency (Stokes) side of each doublet becomes independent of the temperatures, while the high frequency (anti-Stokes) component steadily gets weaker in intensity like $e^{-\hbar\omega/kT}$. Quantum mechanically this results because one can create phonons even at $T=0$; however, the annihilation of phonons is proportional to the number of excited phonons and this number goes to zero as $e^{-\hbar\omega/kT}$ as $T \rightarrow 0$.

We complete the discussion of the intensity and spectral distribution of the Brillouin components by calculating the ξ^μ for the conditions appropriate to our experiments. We studied sound waves propagating in the [110] plane. Thus, \mathbf{k} , \mathbf{k}_0 , and \mathbf{K} were in this plane, and \mathbf{K} could be arranged to make any desired angle φ with respect to the [001] axis lying in this plane. The laser beam was polarized perpendicular to the \mathbf{k} , \mathbf{k}_0 plane. Hence the unit vectors $\mathbf{1}_{\mathbf{E}_0}$ and $\mathbf{1}_{\mathbf{K}}$ have the following components along the cube axes.:

$$\mathbf{1}_{\mathbf{K}} = \left(\frac{\sin \varphi}{\sqrt{2}}, \frac{\sin \varphi}{\sqrt{2}}, \cos \varphi \right), \quad (55)$$

$$\mathbf{1}_{\mathbf{E}_0} = \left(\frac{1}{\sqrt{2}}, -\frac{1}{\sqrt{2}}, 0 \right). \quad (56)$$

The solution of the secular equation³⁶ for the propagation of elastic waves in a cubic crystal shows that the three sound waves which propagate in the direction $\mathbf{1}_{\mathbf{K}}$ have the following polarizations: The first, ($\mu=1$) is a pure transverse wave polarized perpendicular to the \mathbf{k} , \mathbf{k}_0 plane. The second, ($\mu=2$) is a largely transverse wave with appreciable longitudinal admixture for certain values of φ . The third wave ($\mu=3$) is almost entirely a longitudinal wave. The polarization vectors $\hat{\pi}^\mu$ of these waves are

$$\hat{\pi}^1 = \left(\frac{1}{\sqrt{2}}, \frac{-1}{\sqrt{2}}, 0 \right), \quad (57)$$

$$\hat{\pi}^2 = (2 + P_M^2)^{-1/2} (1, 1, P_M), \quad (58)$$

$$\hat{\pi}^3 = (2 + P_L^2)^{-1/2} (1, 1, P_L), \quad (59)$$

where the quantity P_L or P_M is given by

$$P_M^2 = \frac{(\sqrt{2} \cos \varphi \sin \varphi)(C_{12} + C_{44})}{\rho V_M^2 - C_{44} + (\cos^2 \varphi)(C_{44} - C_{11})}, \quad (60)$$

and V_L or V_M is the phase velocity of the primarily longitudinal or mixed polarization mode. Orthogonality of the $\hat{\pi}$'s is assured by the fact that

$$P_L P_M = -2. \quad (61)$$

³⁶ J. DeLauney, *Solid State Physics*, edited by F. Seitz and D. Turnbull (Academic Press Inc., New York, 1956), Vol. 2.

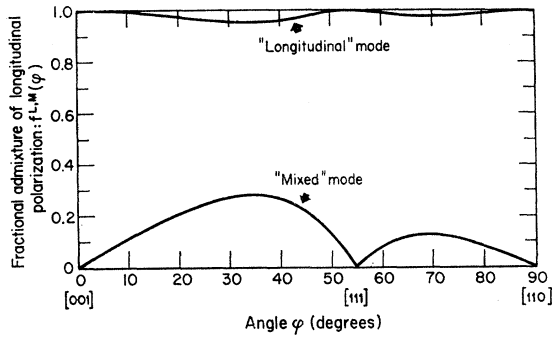


FIG. 2. The fractional longitudinal admixture [$f^L(\varphi)$ and $f^M(\varphi)$] for "longitudinal" and "mixed" acoustic mode phonons propagating in the $[110]$ plane along a direction making an angle φ with the $[001]$ direction.

We now can use Eqs. (55)–(59) in Eqs. (36) and (37) to find the vectors ξ^μ . A simple calculation shows that

$$\xi^1 = (1/2) \left(p_{44} \cos \frac{\theta}{2} - (p_{11} - p_{12} - p_{44}) \sin \varphi \sin \left(\frac{\theta}{2} - \varphi \right) \right) \mathbf{1}_{11}, \quad (62)$$

where θ is the angle between \mathbf{k} and \mathbf{k}_0 and $\mathbf{1}_{11}$ is a unit vector normal to \mathbf{k} lying in the \mathbf{k}, \mathbf{k}_0 plane. Thus the light scattered from the sound wave polarized perpendicular to the $[110]$ plane is polarized in the scattering plane. Also

$$\xi^2 = \left(p_{12} f^M(\varphi) + \frac{(p_{11} - p_{12} - p_{44}) \sin \varphi}{(4 + 2P_M^2)^{1/2}} \right) \mathbf{1}_1, \quad (63)$$

$$\xi^3 = \left(p_{12} f^L(\varphi) + \frac{(p_{11} - p_{12} - p_{44}) \sin \varphi}{(4 + 2P_L^2)^{1/2}} \right) \mathbf{1}_1, \quad (64)$$

where $\mathbf{1}_1 = -\mathbf{1}_{E_0}$. Thus the sound waves polarized in the scattering plane scatter light so that the plane of polarization is perpendicular to the scattering plane. The quantities $f^M(\varphi)$ and $f^L(\varphi)$ represent the fractional longitudinal admixture in the sound wave, i.e.,

$$f^{L,M}(\varphi) = \hat{\pi}^\mu \cdot \mathbf{1}_K = \frac{\sqrt{2} \sin \varphi + (\cos \varphi) P_{L,M}}{(2 + P_{L,M}^2)^{1/2}}. \quad (65)$$

For the primarily longitudinal sound wave $f^L(\varphi)$ is nearly equal to unity for all values of φ . For the mixed mode f^M varies from 0 to a maximum of about 0.3 as φ changes. In Fig. 2 below we plot $f(\varphi)^L$ and $f(\varphi)^M$ for values of the elastic constants appropriate to KI.

It is important to realize that isothermal measurements of the p 's by uniaxial strain studies show that in these alkali halide crystals we may expect that $p_{44} \sim 0.02$, $p_{12} \sim 0.18$ and $p_{11} - p_{12} \sim 0.04$. We therefore expect on examination of Eqs. (62), (63), and (64) that the Brillouin doublets from the longitudinal and mixed

mixed modes will be considerably more intense than the doublet from the purely transverse waves. Our experiment showed this to be the case; in fact we did not see the light scattered from the purely transverse modes. In the analysis of our data we compare the measured relative intensity of the scattering from the mixed and the longitudinal mode with the prediction obtained from Eqs. (63) and (64) using independent measurement of the p 's and find satisfactory agreement.

III. EXPERIMENTAL METHOD

In Fig. 3 we show a schematic diagram of the experimental arrangement for the observation of the spectrum of the scattered light. The light source was a Spectra-Physics Model 115 helium-neon laser which has an output of about 2 mW when operated in the uniphase mode. The laser beam passes through the sample which was mounted in such a way that the collected light is always 90 deg away from the direction of the incident beam. Further, the holder permits the crystal to be rotated so that any direction in a $[110]$ plane can be brought into coincidence with the scattering vector \mathbf{K} . A lens system collects the scattered light and focuses it onto the input slit of a 12-m, high-resolution grating spectrograph. The spectrum of the light is observed by sweeping the position of the exit slit along the focal plane of the spectrograph. The light intensity passing through the exit slit was detected with an RCA 7265 photomultiplier tube whose output was first amplified with a Hewlett-Packard 425-A dc amplifier, and then recorded on a strip chart recorder.

This system is rather straightforward, yet there are certain features which we have found necessary to include which may prove helpful in future work. In particular, attention should be drawn to the problem of passing light through a crystal and collecting the light at say a 90° scattering angle when the faces of the crystal are not normal to the direction of the incident or the scattered light beam. Also, it is well to realize that scattering from a rough crystal surface produces

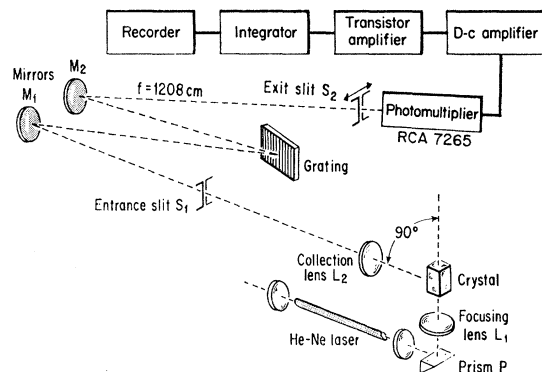


FIG. 3. Experimental arrangement of laser, light focusing and collecting system, grating spectrograph and photoelectric detection chain.

an extremely large amount of scattering at the incident light frequency. In the spectrum this unshifted light has tails which can overlap and mask the Brillouin components. Both these difficulties were circumvented by immersing the crystal in a liquid mixture whose index of refraction can be altered by changing the relative proportion of the constituents until exact match between the liquid and the crystal is achieved. The light enters the scattering cell normal to a glass face of the chamber enclosing the mixture and crystal. The scattered light leaves normal to a second glass face. When match is achieved the crystal seems to disappear in the fluid. This technique is quite helpful, especially when the crystal axes must be rotated into different directions relative to the light beam, as is the case in our experiments. The liquids employed to match our alkali halide crystals were mixtures of di-iodomethane, toluene, and methanol.

Another aspect of our system which merits further comment is the light collection system which involves the focusing lens L_1 , the collection lens L_2 , and the entrance slit S_1 . Because of the low intensity of the Brillouin scattering it is important to arrange these optical elements so as to maximize the light collected without reducing appreciably the resolution of the spectrometer. This can be done as follows. First, the entrance slit width (W) was chosen as large as is consistent with a clear resolution of the Brillouin components. In our case, we chose $W=0.025$ cm which corresponded to $\Delta\nu=1.5$ kMc/sec. The slit height was 1.8 cm. To determine the maximum collectable intensity we return to formulas (17) and (46), and observe that if the illuminated region has the form of a cylinder of length L and a base area A , then the total power collected by a light gathering system having a solid angle Ω is given approximately by

$$P_{\text{col}} \approx P_0 \mathcal{R} L \Omega, \quad (66)$$

where P_0 is the total incident power and \mathcal{R} is the scattering coefficient given by

$$\mathcal{R} = \left(\frac{\omega_0}{c}\right)^4 \frac{\epsilon_0^4}{(4\pi)^2} \left(\frac{kT}{\rho}\right) \sum_{\mu=1}^3 \frac{|\xi^\mu|^2 K^2}{\omega_\mu^2(\mathbf{K})}. \quad (67)$$

We have assumed that the light intensity is uniform in the illuminated cylinder and have taken the axis of the cylinder parallel to the entrance slit. In our system, Ω is the solid angle for the light which is collected by lens L_2 and which subsequently passes through the spectrograph. L_2 forms an image of the source at the slit. Of all the light beams emerging from this image only those inside the spectrograph acceptance solid angle (Ω_0) are collected by the mirror M_1 and pass through the spectrograph. In our spectrograph Ω_0 was 0.68×10^{-4} sr. If M is the magnification of lens L_2 when it forms the image of the source at the slit, then simple geometrical optics shows that Ω and Ω_0 are related by

$$\Omega = M^2 \Omega_0. \quad (68)$$

At first glance it would appear advantageous to make the magnification very large. However, it should be appreciated that this could lead to a situation in which the image of the source could be larger than the slit so that all the collected light would not in fact enter the spectrograph. Thus the collected power is also determined in an important way by the dimensions of the source and the slit. The former dimension is fixed by the focusing lens L_1 which focuses the plane parallel incident laser beam into a double cone whose apex angle is the focal region. This focal region is of primary interest because there the light beam is very narrow and we can magnify it greatly and still have it pass through the entrance slit. The dimensions of the focal region are fixed by diffraction. Analysis of this problem^{37,38} shows that the focal region can be regarded crudely as a bright cylinder of light whose height (h_{so}) and diameter (W_{so}) are given by

$$W_{\text{so}} = \lambda(f/a) \quad (69)$$

$$h_{\text{so}} = 3\lambda(f/a)^2, \quad (70)$$

where f is the focal length of lens L_1 , a is the diameter of the incident laser beam, and λ is the wavelength of light. Let us arrange the source width (W_{so}) always to be of such a size that when magnified by L_2 it always just fills the slit; i.e., we take

$$W_{\text{so}} = (W/M). \quad (71)$$

This requirement fixes the (f/a) ratio of the focusing lens as

$$(f/a) = (W/M\lambda). \quad (72)$$

It also fixes the height of the diffraction-limited region to have the value

$$h_{\text{so}} = (3/\lambda)(W/M)^2. \quad (73)$$

The slit, having a height h , will pass light coming from a region on the source having a height h/M . From Eq. (73) we see that for small M the source height h_{so} is always longer than h/M so that the effective length (L) of the illuminated region to insert into Eq. (66) is $L=h/M$. Using this and Eq. (68) we find that the collected power is linear in M provided that M is not too large, viz:

$$P \approx P_0 \mathcal{R} \Omega_0 M h. \quad (74)$$

This holds true until we reach the magnification M' for which

$$h_{\text{so}} = h/M'. \quad (75)$$

At this value of M the diffraction limited cylinder has the same length to width ratio as does the slit. The magnitude of M' is obtained by using Eqs. (73) and (75). This gives

$$M' = 3W^2/\lambda h. \quad (76)$$

³⁷ M. Born and E. Wolf, *Principles of Optics* (The Macmillan Company, New York, 1964), 2nd ed., pp. 435 ff.

³⁸ Tschunko, J. Opt. Soc. Am. 55, 1 (1965).

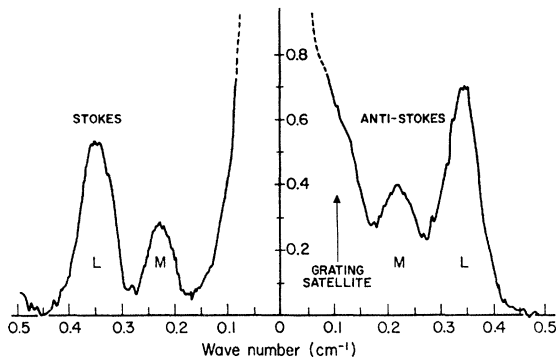


FIG. 4. Recorder tracing of the Brillouin spectrum of light scattered from RbCl. A 22-second integrating time constant was used. The scattering phonons in mixed (M) and longitudinal (L) branches were propagating along a direction 40° away from the $[001]$ direction in a $[110]$ plane. The strong central or "elastic" component results from scattering off imperfections in the crystal. It is asymmetrical because of grating irregularities.

With our initial choice of slit width $M' \simeq 15$. For $M > M'$ the diffraction limited cylinder is shorter than the demagnified image of the slit and the collected power continues to rise, but much more slowly than linearly in M . Thus the focal length of lens L_1 is chosen to satisfy Eq. (72) with $M = M'$, and the focal length and position of lens L_2 is chosen so that it focuses the source at the slit with magnification M' . It can be shown that the resulting acceptance solid angle $\Omega = M'^2 \Omega_0$ is not large enough to artificially broaden the Brillouin components by accepting too large a range in scattering angle.

The grating used for spectral analysis of the collected light was ruled under interferometric control in Dr. G. Harrison's laboratory at MIT. The grating dimensions were 5 in. \times 10 in. with 300 lines/mm and the grating was blazed at 63.5° . To obtain sufficiently large dispersion the grating was used in the tenth order at an angle of 72° . The resolving power of the grating was $\sim 750\,000$.

The crystals studied were KCl, RbCl, and KI. The first two were provided by Professor A. Smakula. The last sample was obtained from the Harshaw Chemical Company. The samples were typically cubical in shape with $\sim \frac{1}{2}$ in. on an edge. Of the available samples we consistently chose those which, when illuminated by the laser beam, showed the greatest clarity and freedom from inclusions. Inclusions in the crystal produce a large elastic scattering of the light. If there are enough such scattering centers they can produce a central component in the spectrum whose tails have more intensity than the Brillouin components. Thus a selection of clear samples is especially important in resolving the Brillouin spectrum.

The index of refraction of each of these crystals is well known³⁹ at 6328 \AA .

³⁹ Landolt-Börnstein, *Zahlenwerte und Funktionen aus Physik-Chemie-Astronomie-Geophysik-Technik* (Springer-Verlag, Berlin, 1962), 6th ed., Vol. II, Part A, Chap. 8.

IV. EXPERIMENTAL RESULTS

Using the methods discussed in Sec. III we measured the Brillouin spectrum of light scattered 90° away from the incident direction. For this scattering angle, the wavelength λ_s of the scattering phonon is

$$(2\pi/\lambda_s) = \sqrt{2}(n\omega_0/c),$$

in accordance with Eq. (13). This wavelength is the same for all orientations of the crystal axes and has the values $\lambda_s = 3007.4 \text{ \AA}$, 2999.9 \AA , and 2694.5 \AA , respectively, for KCl, RbCl, and KI. For each orientation of the crystal at least 10 traces of the Brillouin spectrum were taken. An example of such a trace is shown in Fig. 4. This trace shows clearly the scattering from both longitudinal (L) and mixed (M) longitudinal and transverse acoustic branches. The grating itself produced spurious Rowland ghosts and satellite lines whose position and relative intensity was accurately determined by sweeping out a spectrum of the laser itself. The spurious lines were removed by making a point-by-point subtraction on each trace. This subtraction procedure, while laborious, was especially important in accurately resolving the lines coming from relatively weak mixed acoustic modes.

The frequency difference $\nu - \nu_0$ between the Brillouin components and the laser frequency gives the frequency of the scattering phonon. The phase velocity of the scattering phonon is obtained from Eq. (15). This procedure was carried out as a function of φ the angle between the $[001]$ direction and the sound wave propagation direction in the $[110]$ plane. In Table I we give the sound-wave frequency ($\nu - \nu_0$) and the phase velocity V as a function of the angle φ for each of the observable acoustic modes of KCl. In Tables II and III we present the corresponding results for RbCl and KI.

In Figs. 5, 6, and 7 we present plots of the sound velocity V in the $[110]$ plane as a function of the angle φ for the longitudinal and mixed branches of the acoustic sound waves. The third acoustic branch consists of pure transverse waves from which we observed no Brillouin scattering. In KCl, where the

TABLE I. Frequency and phase velocity of sound waves of 3007 \AA wavelength as a function of propagation direction in the $[110]$ plane in KCl.

Angle φ (deg)	Sound wave frequency $\nu - \nu_0$ (kMc/sec)	Phase velocity V (m/sec)	Acoustic mode designation	Temperature ($^\circ\text{C}$)
0	15.00 ± 0.1	4509 ± 35	L	22.7
25	14.1 ± 0.1	4237 ± 38	L	22.6
35	13.3 ± 0.1	3995 ± 30	L	22.7
	8.1 ± 0.1	2446 ± 34	M	22.7
45	12.45 ± 0.08	3745 ± 25	L	22.7
55	12.12 ± 0.06	3645 ± 20	L	22.8
70	12.57 ± 0.06	3780 ± 18	L	22.6
90	12.93 ± 0.06	3889 ± 19	L	23.1

TABLE II. Frequency and phase velocity of sound waves of 3000 Å wavelength as a function of propagation direction in the [110] plane in RbCl.

Angle φ (deg)	Sound wave frequency $\nu - \nu_0$ (kMc/sec)	Phase velocity V (m/sec)	Acoustic mode designation	Temperature (°C)
0	12.15±0.07	3646±21	L	23.1
25	11.42±0.06	3426±18	L	22.5
	5.84±0.1	1752±31	M	22.5
30	11.10±0.07	3331±21	L	22.5
	6.21±0.16	1863±50	M	22.5
35	10.72±0.07	3216±21	L	22.5
	6.46±0.09	1939±30	M	22.5
40	10.33±0.07	3099±20	L	22.8
	6.75±0.2	2025±47	M	22.8
45	10.10±0.07	3030±20	L	22.3
	6.75±0.18	2025±53	M	22.3
55	9.80±0.05	2940±16	L	22.4
70	10.19±0.06	3058±16	L	22.4
90	10.51±0.06	3153±18	L	22.4

scattering intensity was low even for the longitudinal waves, and the scattering from crystal imperfections produced a particularly strong central component, we were able to find scattering from the mixed mode only for $\varphi = 35^\circ$. In RbCl and KI however, we have data on the velocity in the mixed mode for five different angles φ .

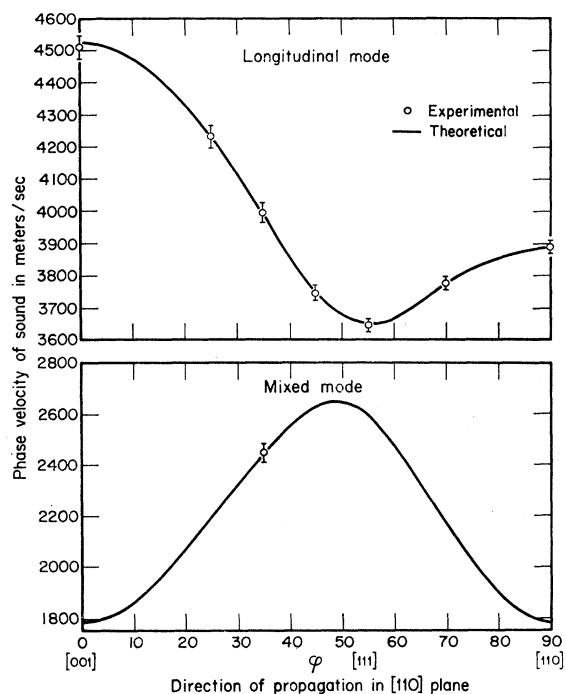


FIG. 5. The phase velocity of sound waves in KI with wavelength 3007.4 Å as a function of propagation direction in the [110] plane. The upper graph gives the velocity of the longitudinal acoustic mode. The lower graph gives the velocity of the mixed mode. No scattering from the purely transverse acoustic mode was detected. The solid lines represent the theoretical variation of velocity using the values of hypersonic elastic constants given in the text.

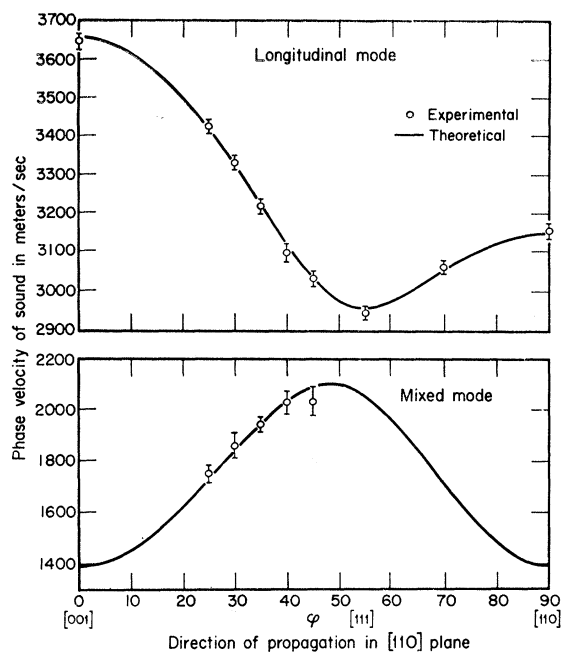


FIG. 6. The phase velocity of sound waves in RbCl with wavelength 3000.0 Å as a function of propagation direction in the [110] plane. The upper graph gives the velocity of the longitudinal acoustic mode. The lower graph gives the velocity of the mixed mode. No scattering from the purely transverse acoustic mode was detected. The solid lines represent the theoretical variation of velocity using the values of hypersonic elastic constants given in the text.

We also have information on the intensity of the Brillouin components in the scattered light. The scattering from KI was the strongest. RbCl and KCl both produce a scattering intensity about half that of KI. In Table IV we give the ratio of the peak amplitudes (A) of the longitudinal Brillouin peaks in these crystals for several directions in the [110] plane. It is

TABLE III. Frequency and phase velocity of sound waves of 2694.5 Å wavelength as a function of propagation direction in the [110] plane in KI.

Angle φ (deg)	Sound wave frequency $\nu - \nu_0$ (kMc/sec)	Phase velocity V (m/sec)	Acoustic mode designation	Temperature (°C)
0	11.05±0.06	2978±16	L	22.6
15	10.74±0.07	2893±17	L	22.6
25	10.16±0.07	2736±19	L	22.5
	5.24±0.09	1412±24	M	22.5
30	9.81±0.06	2644±17	L	22.3
	5.57±0.07	1500±18	M	22.3
35	9.49±0.06	2558±16	L	22.3
	5.81±0.06	1565±17	M	22.3
40	9.13±0.04	2460±12	L	22.4
	6.07±0.08	1635±21	M	22.4
45	8.90±0.05	2400±13	L	22.5
	6.33±0.12	1707±33	M	22.5
55	8.64±0.05	2328±12	L	22.4
65	8.83±0.04	2379±11	L	22.2
75	9.09±0.04	2448±11	L	22.4
90	9.26±0.04	2494±11	L	22.6

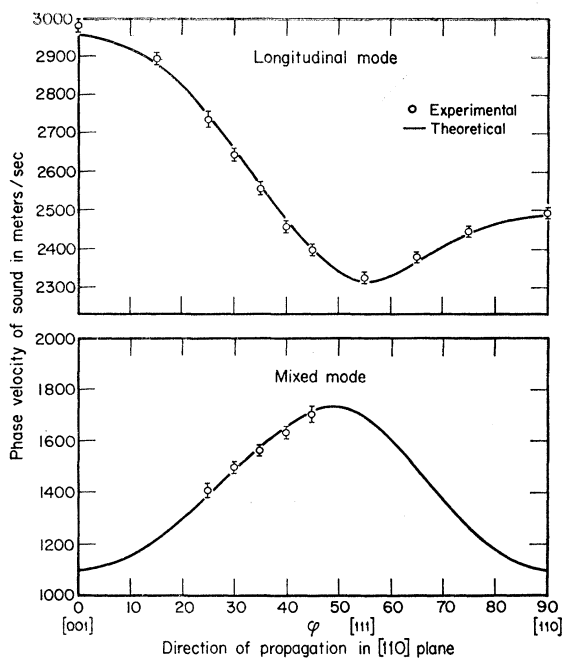


FIG. 7. The phase velocity of sound waves in KI with wavelength 2694.5 Å as a function of propagation direction in the [110] plane. The upper graph gives the velocity of the longitudinal acoustic mode. The lower graph gives the velocity of the mixed mode. No scattering from the purely transverse acoustic mode was detected. The solid lines represent the theoretical variation of velocity using the values of hypersonic elastic constants given in the text.

informative to compare the scattering intensity from solids with that from liquids.²⁰ The peak amplitudes of the scattering from toluene, water, and KCl stand in the ratio 32:10:1.

In Fig. 8 we give data on the relative amplitude of the scattering from the mixed modes and the longitudinal mode as a function of the propagation direction in the [110] plane for RbCl and KI. The angles φ for which we could observe the mixed mode ranged from 25° to 45° in both these crystals. When φ is less than 25° the mixed mode velocity is small enough so that this peak begins to merge into the central peak and is therefore difficult to resolve. For φ greater than 45° the intensity of this mode falls so low that it could not be detected.

V. THEORETICAL ANALYSIS

The measurements presented in the previous section give the phase velocity ($\omega_\mu/|\mathbf{q}|$) of the acoustic vibrations as a function of the propagation direction. In the

TABLE IV. Relative peak amplitudes of "longitudinal" Brillouin components in KCl, RbCl, and KI for selected directions of sound propagation.

$A_{\text{KCl}}:A_{\text{RbCl}}:A_{\text{KI}}$	[001]	[111]	[110]
	1.0:1.0:2.7	1.0:1.3:2.0	1.0:1.1:1.7

present section we consider the theoretical predictions for the magnitude and angular dependence of this velocity. We shall also consider briefly the extent to which the theory of the intensity as given in Sec. II is consistent with the observed scattering intensities.

The theory of lattice vibrations is well established. It is known⁴⁰ that the dispersion relation which links the vibration frequencies for each mode (μ) to the wave vector \mathbf{q} of the wave is obtained by diagonalizing the so-called dynamical matrix. The elements of this matrix are related directly to the atomic force constants. These describe the force exerted on a given atom when it, or any other atom in the lattice, is displaced from its equilibrium position. It is also well known⁴⁰ that when the wavelength of the lattice vibration is very long compared to the interatomic distances the dispersion relation takes the simple form

$$\omega_\mu(\mathbf{q}) = V(\mathbf{l}_q) |\mathbf{q}|, \quad (77)$$

where the velocity V is a function only of the direction of propagation. In this limit the solid behaves like an elastic continuum and the dynamical matrix for the vibrations can be written⁴⁰ in terms of the elastic constants rather than the interatomic force constants.

In our experiments the wavelength of the sound waves is about 1000 times longer than the lattice spacing. We therefore expect that the solid can be treated as an elastic continuum. We shall take this as

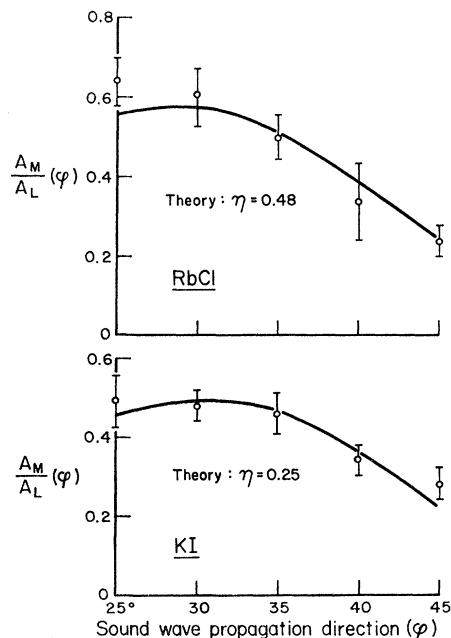


FIG. 8. The ratio of the maximum amplitudes of the mixed mode and the longitudinal mode Brillouin components (A_M/A_L) as a function of the direction of propagation (φ) in the [110] plane for KI and RbCl.

⁴⁰ A. A. Maradudin, E. W. Montroll, and G. Weiss, *Theory of Lattice Dynamics in the Harmonic Approximation* (Academic Press Inc., New York, 1963).

TABLE V. Hypersonic and ultrasonic values of the elastic constants of KCl.

Wavelength (Å)	Frequency (cps)	Temperature (°C)	C_{11}	C_{44}	C_{12} (10^{11} dyn/cm ²)	$2C_{44}+C_{12}$
3007	$8-15 \times 10^9$	22.8	4.06 ± 0.01	0.63 ± 0.01	0.69 ± 0.04	1.95 ± 0.02
$\sim 5 \times 10^6$	$\sim 9 \times 10^6$	22	4.078 ± 0.008^a	0.633 ± 0.006^a	0.69 ± 0.014^a	1.96 ± 0.03^a

^a S. Haussühl, Z. Physik 159, 223 (1960).

the basis of our analysis, and at the end we shall examine the degree to which the experimental results are consistent with this assumption.

In a cubic crystal the elastic strain produced by a small stress can be described by three elastic constants, C_{11} , C_{12} , and C_{44} . The dynamical matrix for the sound waves in a cubic crystal is well known.³⁶ The eigenvalues and eigenvectors of this matrix give, respectively, the sound velocity and polarization of each of the three orthogonal waves in the acoustic branches. For waves which propagate in a [110] plane one acoustic wave (T) is polarized purely transverse to the propagation direction. One wave (L) is largely longitudinal and one (M) has a mixed polarization both along and perpendicular to \mathbf{q} . The velocity of each of these three waves is given below as a function of the propagation direction φ in the [110] plane. (φ is the angle between [001] and the direction of propagation.)

$$V_T(\varphi) = (1/2\rho)^{1/2} [(C_{11} - C_{12}) + (\cos^2 \varphi)(2C_{44} + C_{12} - C_{11})]^{1/2}, \quad (78)$$

$$V_L(\varphi) = (1/4\rho)^{1/2} \{ (4C_{44} + C_{11} + C_{12}) - (\cos^2 \varphi)(2C_{44} + C_{12} - C_{11}) + [(C_{11} + C_{12})^2 + (2C_{44} + C_{12} - C_{11}) \times (\cos^2 \varphi)(8C_{44} + 14C_{12} + 6C_{11}) - (\cos^4 \varphi)(6C_{44} + 15C_{12} + 9C_{11})]^{1/2} \}^{1/2}, \quad (79)$$

$$V_M(\varphi) = (1/4\rho)^{1/2} \{ [(4C_{44} + C_{11} + C_{12}) - (\cos^2 \varphi)(2C_{44} + C_{12} - C_{11}) - [(C_{11} + C_{12})^2 + (2C_{44} + C_{12} - C_{11}) \times (\cos^2 \varphi)(8C_{44} + 14C_{12} + 6C_{11}) - (\cos^4 \varphi)(6C_{44} + 15C_{12} + 9C_{11})]^{1/2}]^{1/2}, \quad (80)$$

where ρ is the mass density.

It may be helpful to mention the fact that the sum of the squares of the velocity of sound waves moving in

any direction in the crystal is a constant given by

$$\sum_{\mu=1}^3 \rho V_{\mu}^2 = C_{11} + 2C_{44}. \quad (81)$$

Along the direction of principal symmetry in the [110] plane, namely the [001], the [111] and the [110] directions, ρV_L^2 takes on the values C_{11} , $[2(2C_{44} + C_{12}) + C_{11}]/3$, $[2C_{44} + C_{12} + C_{11}]/2$, respectively. Away from these directions the velocity in the longitudinal branch still depends only on C_{11} and the combination $(aC_{44} + bC_{12})$ where a is nearly 2 and b is nearly 1. Thus, from our measurements on this branch we can obtain accurately the two quantities C_{11} and $2C_{44} + C_{12}$. In the mixed mode ρV_M^2 takes on the values C_{44} , $(C_{44} + C_{11} - C_{12})/3$ and C_{44} , respectively, in the directions [001], [111], and [110]. We found the velocity in this mode only between $25^\circ < \varphi < 45^\circ$. In this angular region the velocity is fairly sensitive to C_{44} and an initial choice of C_{44} could be made from a single value of the velocity in the branch. To determine the elastic constants more accurately, we started with the elastic constants obtained from the sound speeds in three different directions. About these values we constructed a net of possible values for each of the three elastic constants. Using Eqs. (79) and (80) and an IBM 709 computer, we calculated the velocity of sound in each observed direction for each triplet in the net. The computer also found for each triplet the mean square deviations between the theoretical and experimental values of velocity. The values of C_{11} , C_{12} , C_{44} , and $2C_{44} + C_{12}$ which showed the minimum deviation between theory and experiment are given in the first row of Tables V, VI, and VII along with their estimated error limits. In the second row of each table we list the results of recent accurate measurements⁴¹ of these elastic constants in KCl and KI. These measurements were made on sound waves generated by an acoustic transducer operating in the 9-Mc/sec frequency region. Our

TABLE VI. Hypersonic and ultrasonic values of the elastic constants of RbCl.

Wavelength (Å)	Frequency (cps)	Temperature (°C)	C_{11}	C_{44}	C_{12} (10^{11} dyn/cm ²)	$2C_{44}+C_{12}$
3000	$6-12 \times 10^9$	22.6	3.74 ± 0.01	0.535 ± 0.02	0.72 ± 0.04	1.79 ± 0.02
$\sim 2 \times 10^6$	10 and 20×10^6	22	3.72 ± 0.06^a	0.503 ± 0.01^a		

^a C. Garland and R. Young (private communication).

⁴¹ S. Haussühl, Z. Phys. 159, 223 (1960).

TABLE VII. Hypersonic and ultrasonic values of the elastic constants of KI.

Wavelength (Å)	Frequency (cps)	Temperature (°C)	C_{11}	C_{44} (10^{11} dyn/cm ²)	C_{12}	$2C_{44}+C_{12}$
2695	$(5-11)\times 10^9$	22.4	2.73 ± 0.01	0.375 ± 0.015	0.40 ± 0.03	1.15 ± 0.02
$\sim 3\times 10^6$	$\sim 9\times 10^6$	22	2.76 ± 0.006^a	0.37 ± 0.004^a	0.45 ± 0.01^a	1.19 ± 0.02^a

^a S. Haussühl, Z. Physik 159, 223 (1960).

measurements correspond to sound waves which have a constant wavelength (~ 3000 Å) regardless of the direction of propagation in the crystal. The wavelengths and frequencies involved in both types of measurement are also given in these tables.

From these tables we observe that in KCl and KI the hypersonic and the ultrasonic values of the elastic constants are in excellent agreement. This indicates the absence of dispersion in the sound velocity between 10 Mc/sec and ~ 10 kMc/sec for these crystals.

In the case of RbCl, Professor C. Garland and R. Young at MIT kindly carried out a measurement of C_{11} and C_{44} for our sample using an acoustic echo method. The results of their measurement are shown in Table VI. Comparison between the ultrasonic and hypersonic values shows that in this case as well there is no detectable dispersion in the velocity on increasing the sound wave frequency from ~ 20 Mc/sec to ~ 10 kMc/sec.

We also observe that the Brillouin scattering measurements of the C 's have a precision (~ 0.25 – 4.0 percent) which is about two to three times poorer than these very good ultrasonic measurements. We feel that the use of higher resolution optical spectrometers such as the Fabry-Perot etalon⁴² and higher power lasers will permit an increase in precision in the Brillouin scattering measurements by a factor of 3–5.

In Figs. 5, 6, and 7 we plot as solid lines the theoretical angular variation of the velocity in the "longitudinal" and "mixed" modes using the elastic constants given in Tables V, VI, and VII. The agreement between the theoretical and experimental values is excellent: The theoretical values agree with the experimental values generally well within the experimental limit of error of $\sim 0.5\%$ for the longitudinal mode and $\sim 2\%$ for the "mixed" mode.

As a final part of our analysis of the data we examine theoretically the results on the relative amplitude of the scattering from the mixed mode and the longitudinal mode. If the slit width of the spectrograph is broad compared with the natural linewidth of the Brillouin component, then the measured maximum amplitude of the signal as observed at the output slit is proportional to the total intensity under the Brillouin component. Under these conditions, which apply in our experiments, the observed ratio A_M/A_L is given in

accordance with Eqs. (17), (46), (63), and (64) by

$$(A_M/A_L) = (\omega_L \xi^2 / \omega_M \xi^3)^2 = (V_L \xi^2 / V_M \xi^3)^2, \quad (82)$$

where V_L and V_M are the velocities of the longitudinal and mixed mode sound waves, respectively. From Eqs. (63) and (64) we may write the angular dependence of A_M/A_L as

$$\frac{A_M}{A_L} = \left[\frac{V_L(\varphi)(f^M(\varphi) + \eta \sin \varphi / (2 + P_M^2)^{1/2})^{-2}}{V_M(\varphi)(f^L(\varphi) + \eta \sin \varphi / (2 + P_L^2)^{1/2})} \right]^2, \quad (83)$$

where

$$\eta = (p_{11} - p_{12} - p_{44}) / \sqrt{2} p_{12}, \quad (84)$$

and P_L and P_M are given as functions of the phonon direction by Eq. (60). The velocities V_L and V_M are known as a function of φ from our measurements. The quantities $f^M(\varphi)$ and $f^L(\varphi)$ represent the known fractional longitudinal admixture in the sound wave as defined in Eq. (65). To calculate theoretically the magnitude of A_M/A_L for each direction of propagation all that is needed is the value of the parameter η . If we chose the value $\eta = 0.48$ for RbCl and $\eta = 0.25$ for KI we obtain the values for A_M/A_L given as a solid line in Fig. 8.

Burstein and Smith⁴³ have measured p_{11} and p_{12} in KI. They also have measured p_{11} , p_{12} , and p_{44} in KBr while Pockels⁴⁴ has measured these in KCl. These measurements suggest that $p_{44} \cong -0.026$ for all three potassium halides. Using this and⁴³ $p_{11} = 0.21$, $p_{12} = 0.17$ we find $\eta = 0.27$ for KI. This is in excellent agreement with the experimental value of $\eta = 0.25$. No experimental data exists on the p 's for RbCl, but the value of $\eta = 0.48$ seems reasonable in view of the fact that the scattering from RbCl is about twice as small as that from KI. This suggests that p_{12} is a factor of 2 smaller for this crystal and that correspondingly η could be 2 times bigger.

ACKNOWLEDGMENTS

The authors wish to thank Professor A. Smakula and J. Kalnajs for providing the polished crystals of KCl and RbCl, and T. Greytak for help with the computer program used in finding the microwave elastic constants. We also thank J. B. Lastovka for advice and help.

⁴³ E. Burstein and P. L. Smith, Phys. Rev. 74, 229, 1880 (1948).

⁴⁴ F. Pockels, Lehrbuch der Kristallographie (Teubner, Leipzig, 1906), p. 467.

⁴² P. Jacquinet, Rept. Progr. Phys. 23, 267 (1960).